COBEM 2023 27TH INTERNATIONAL CONGRESS OF MECHANICAL ENGINEERING

ABCM Brazilian Society of Mechanical Sciences and Engineering
27th ABCM International Congress of Mechanical Engineering
December 04-08, 2023, Florianópolis-SC, Brazil

COB-2023-1025
NUMERICAL CHARACTERIZATION AND ANALYSIS OF THE CHEMICAL KINETICS OF THE MIXTURE OF SILANE, HYDROGEN AND AIR FOR SUPERSONIC COMBUSTION APPLICATIONS

Rafael Maia Altafim
Loreto Pizzuti
Alexandre Costa Goulart
Federal University of ABC, Santo Andre – SP , Brazil
r.altafim@aluno.ufabc.edu.br
loreto.pizzuti@ufabc.edu.br
a.goulart@aluno.ufabc.edu.br

Abstract. *Supersonic combustion engines, known as scramjets, are used in hypersonic vehicles, which fly at speeds above Mach 5.0. The study of hypersonic technology has been carried out by the main militarily developed nations in the world due to the inability of the defense systems currently in operation to protect their territory from vehicles flying at this speed. Among other countries, the Brazilian Air Force are currently working on the development of the project for the Brazilian Hypersonic Vehicle 14-X. In this context, the purpose of this article is to develop a theoretical characterization of the mixture of silane (SiH_4), hydrogen (H_2) and air (O_2 ,N_2) performing a chemical kinetics analysis for supersonic combustion application. Therefore, this analysis will consider the altitude of 30 km to gather the concentration of oxygen and nitrogen gases in atmospheric air, considering that this is a cruise altitude of supersonic combustion engines. The analysis utilizes the silane_v2 mechanism, developed by Miller in 2004, for the silane-hydrogen-air mixture. A reduced mechanism with enhanced computational efficiency was developed, called silane_v3. This new mechanism also adds the chemical transport elements properties which were estimated for accurate modeling, and equations from the GRI Mech 3.0 mechanism were incorporated for NOx pollutant emission analysis. Therefore, the characterization should determine the ignition delay time of the combustion, the laminar flame speed and the concentration of the combustion products, including pollutants species, for different mixture compositions of silane, hydrogen and air.*

Keywords: *silane, hydrogen, supersonic combustion, laminar flame speed, ignition delay time*

1. INTRODUCTION

Supersonic combustion engines, commonly known as scramjets (supersonic combustion ramjets), play a critical role in the propulsion systems of hypersonic vehicles. These engines are specifically designed to operate at speeds surpassing Mach 5.0, where traditional jet engines face challenges in terms of feasibility (Anderson, 2020). The advancement of supersonic combustion technology has attracted substantial attention from militarily advanced nations and aerospace organizations worldwide.

Hypersonic vehicles powered by scramjets have various military and civilian applications. In the military domain, they can serve as strategic weapons delivery platforms, enabling rapid and precise global strike capabilities (Cone, 2019). In addition, the existing defense systems in operation are currently incapable of effectively safeguarding against these advanced hypersonic platforms (Kraska, 2022).

Several countries, including Brazil, have recognized the strategic importance of hypersonic technology and are actively engaged in its development. The Brazilian Air Force is currently involved in the Brazilian Hypersonic Vehicle 14-X Project (Fig. 1), which aims to design and develop a hypersonic vehicle capable of operating at speeds above Mach 5.0 (FAB, 2021). The successful realization of such project has the potential to reshape aerospace capabilities, providing nations with enhanced military capabilities and opening up new possibilities for commercial aviation.

In this context, the purpose of this article is to conduct a comprehensive theoretical analysis of the chemical kinetics involved in the mixture of silane (SiH_4), hydrogen (H_2) as fuel, and air (O_2, N_2) as oxidant for the application of supersonic combustion. This research aims to provide a detailed characterization of the combustion process by examining the reaction kinetics and species concentration in the given mixture. By employing chemical kinetics analysis, the study seeks to explore the ignition delay time, laminar flame speed and the concentration of combustion products, including pollutant species in the conditions of pressure and temperature of the studied scramjet engine.

Figure 1. Artistic Conception of the Brazilian Hypersonic Vehicle 14-X (FAB, 2021).

2. METHODOLOGY

The methodology section of this article provides a comprehensive description of the supersonic engine under investigation. Furthermore, the study outlines the global reaction equation governing the combustion process of the silane and hydrogen mixture with atmospheric air, considering the complex interactions among the fuel components and oxidizer species. To accurately capture the intricate chemical kinetics involved, a carefully formulated chemical kinetics mechanism is employed. This mechanism is based on fundamental principles and incorporates detailed reaction pathways and rate constants, enabling a thorough analysis of the combustion behavior.

2.1 Motor characteristics

Considering that the supersonic engine operates as an air-breathing propulsion system and relies on atmospheric oxygen for combustion, its functionality is contingent upon specific operational conditions required to attain velocities exceeding Mach 5. However, due to the challenges associated with achieving such high speeds, an auxiliary propulsion method becomes necessary to initiate the acceleration process. This can be achieved through the utilization of an accelerator vehicle equipped with either rocket or jet engines.

Additionally, considering the atmospheric air density, the altitude chosen for hypersonic flight in this research is set at 30 km. This altitude selection is based on its relevance in obtaining accurate motor parameters, as reported by Bezzera (2020) and Carneiro (2020) (see Tab. 1). By conducting the analysis at this specific altitude, the study aims to capture the conditions that closely resemble real-world hypersonic flight scenarios and provide valuable insights into the performance and behavior of the engine under such operating conditions.

Table 1. Motor Parameters at Altitude of 30 km.

Motor Parameters	**Values**
Combustion Chamber Pressure	1 atm
Combustion Chamber Temperature	1100 K
Combustion Chamber Mach	2.2
Air Flow Mach	6.5

2.2 Global combustion reaction

The combustion reaction under investigation is defined by a mixture comprising 20% silane with hydrogen gas. According to Jachimowski (1983), concentrations of silane above 10% exhibit a thermal effect on the reaction, contributing to the combustion of hydrogen. However, higher concentrations of silane have a negligible impact on the ignition delay time. Consequently, McLain et al. (1983) adopted a concentration of 20% for the analysis of silane as an initiator for hydrogen combustion.

Furthermore, it is observed that the concentration of oxygen and nitrogen in the atmosphere does not exhibit significant variation up to an altitude of 100 kilometers, as indicated by the atmospheric model MSIS-E-90 developed by NASA. Therefore, the adopted proportion of atmospheric gases is 21% O2 and 79% N2.

Hence, considering the specified concentrations of silane, hydrogen, oxygen, and nitrogen gases, as described above, the fuel and air concentration mixture can be represented by Eq. (1).

$$x\,H_2 + y\,SiH_4\; z\,O_2 + 3{,}76z\,N_2 \tag{1}$$

Since, $x = H_2$ concentration; $y = x\left(\frac{f}{1-f}\right)$; and, $z = \frac{\frac{1}{2}x+2y}{\Phi}$, where f is the percentage of SiH_4 in fuel mixture and Φ is the fuel-air equivalence ratio.

Equation (1) will yield the molar concentration composition for each element of the combustion mixture, which will serve as input for the silane_v3 kinetics mechanism described at the next subsection. The accurate determination of molar concentrations is essential for obtaining reliable results in the investigation of these combustion characteristics. By utilizing this equation, the study aims to obtain a comprehensive understanding of the composition of the mixture and its influence on the ignition delay and flame propagation behavior.

2.3 Kinetics mechanism

The base mechanism used for the analysis is the Silane_v2 mechanism, developed by Miller in 2004. It consists of 68 species and 198 reactions specifically designed for the silane-hydrogen-air mixture. To facilitate its implementation in Python for chemical kinetics analysis, the Silane_v2 mechanism was converted into the Cantera format (Silane_v2.yaml).

Additionally, to reduce computational processing time while still capturing the essential combustion behavior, a reduced mechanism was developed. This reduced mechanism includes 34 species and 70 reactions, offering a more efficient approach to the analysis for simplifying studies of the combustion process.

In addition, equations related to the NO and NO2 species, extracted from the GRI Mech 3.0 mechanism, were incorporated to enable the analysis of pollutant emissions. These equations provide a detailed representation of the chemistry involved in the formation and transformation of nitrogen oxides (NOx) during the combustion process.

By incorporating the Silane_v2 mechanism, utilizing the Cantera software, employing a reduced mechanism, and considering estimated transport properties, a new mechanism, named Silane_v3, was developed. This updated mechanism and has a total of 37 species and 74 reactions described at Appendix A and aims to provide a comprehensive analysis of the chemical kinetics of the silane-hydrogen-air system.

To ensure accurate representation of the transport properties of the silane species, the transport values were estimated based on the Transport Property Table from the University of San Diego, 2023. These values play a crucial role in precisely modeling the transport phenomena within the mixture, enabling a deeper understanding of the supersonic combustion process and its potential applications. The transport properties of the estimated species showed at Appendix B was based on the multiplication of the proportion given by the following species showed at Tab. 2.

Table 2. Transport Properties baseline to Estimation.

Species	**Diameter**	**Well-depth**
CH4	3.746	141.40
CH3	3.800	144.00
CH	2.750	80.00
Mean Hydro carbonate ($\overline{CH}$)	3.432	120.47
SiH4	4.084	207.60
SiH3	3.943	170.00
SiH	3.662	95.80
Mean Hydro silane ($\overline{SiH}$)	3.896	157.8
Proportion between Means to Estimation SIH / CH	13.52 %	29.55 %

Moreover, the integration of these methodologies and data sources enables a detailed investigation into the combustion characteristics. It contributes to the estimation of the laminar flame speed for this fuel mixture, which lacks experimental data due to the complex and challenging nature of spontaneous combustion of silane with air.

2.4 Validating Silane_v3 mechanism

The validation of a chemical kinetics mechanism is important in the field of combustion research. It serves as a crucial step in ensuring the accuracy and reliability of the mechanism's predictions and its applicability to real-world scenarios.

In this study, the validation of the Silane_v3 mechanism will be carried out to assess its performance and predictive capabilities. The validation process will involve comparing the mechanism's predictions with experimental data of ignition delay time, which provides valuable insights into the time required for the onset of combustion.

Additionally, the indirect evaluation of the laminar flame speed attribute will also be employed to validate the mechanism. Laminar flame speed is a critical parameter that characterizes the propagation of a flame front and is often used to assess the combustion performance of a fuel mixture.

Through this comprehensive validation approach, the reliability and accuracy of the Silane_v3 mechanism will be assessed, ensuring its suitability for analyzing the combustion characteristics of the silane-hydrogen mixture in supersonic motor conditions.

2.4.1 Ignition delay time

For the validation of the mechanism using the ignition delay parameter, the reference data provided by Miller was utilized. Moreover, the validation was conducted by comparing the calculated ignition delay times of the Silane-based mixtures with the experimental data from McLain. Two different mixture compositions, referred to as Mixture A and Mixture B, were considered for the analysis.

Mixture A consisted of 2% SiH4, 8% H2, 4% O2, and 86% N2, while Mixture B comprised 1.68% SiH4, 6.72% H2, 6.74% O2, and 84.86% N2 as shown in Fig. 2 the calculated by Silane_v3 mechanism. These compositions were selected to represent different fuel-to-oxidizer ratios and simulate realistic conditions for the Silane-based fuel system.

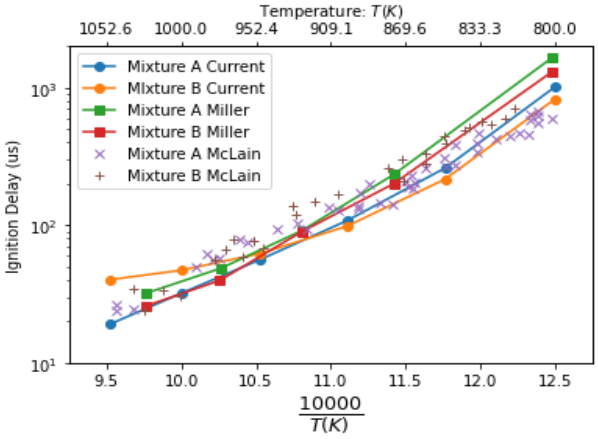

Figure 2. Temperature versus the Ignition Delay Time of silane_v3, Miller mechanism and McLain experimental data to fuel mixture A and B.

By comparing the calculated ignition delay times of Mixture A and Mixture B with the corresponding experimental data, the accuracy and reliability of the Silane_v3 mechanism in predicting ignition characteristics can be assessed. This validation process is crucial for ensuring the credibility and applicability of the developed mechanism in studying the combustion behavior of Silane-based fuel systems.

2.4.2 Laminar flame speed

The validation of the mechanism using the laminar flame speed parameter was made in two steps. The first step was to compare the laminar flame speed of H2-air reported by Dong 2010 showed in the Fig. 3 with the calculated by the Silane_v3 showed in the Fig. 4.

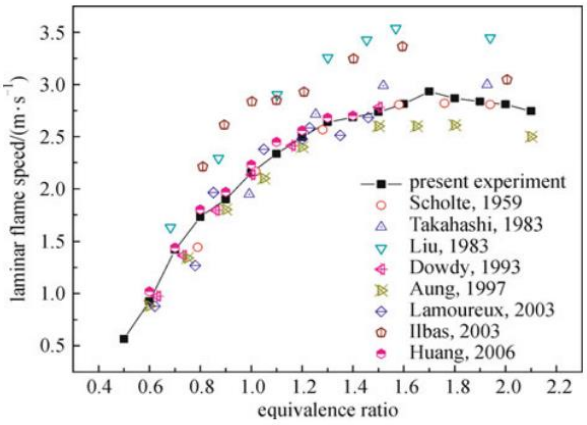

Figure 3. Laminar flame speed of H2/air versus equivalence ratio by Dong 2010.

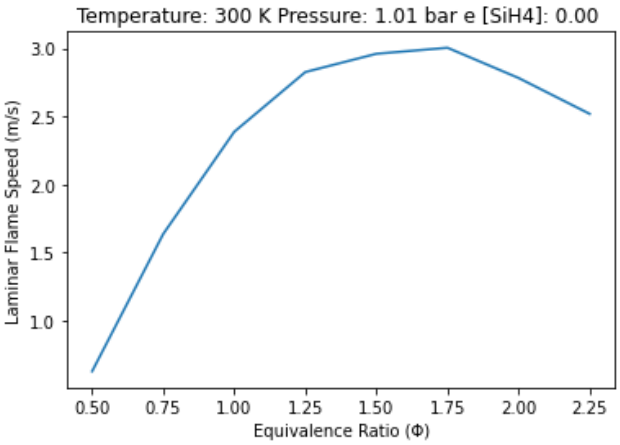

Figure 4. Laminar flame speed of H2/air versus equivalence ratio from Silane_v3.

Secondly, the validation of the developed chemical kinetics mechanism in this project also involved the assessment of the flame extinction velocity of the silane, hydrogen, and air mixture through the laminar flame speed of hydrocarbons and H2, as reported by Pellet in 1991 and 2007.

Figure 5 illustrates the blow off characteristic of the mixture of silane and hydrogen diluted in nitrogen solution, while Fig. 6 represents the laminar flame speed of various hydrocarbon fuels.

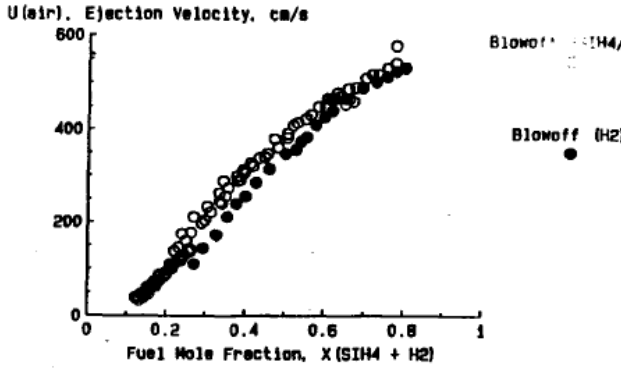

Figure 5. Blow off characteristics of nitrogen diluted 20% silane/H2 (Pellett,1991).

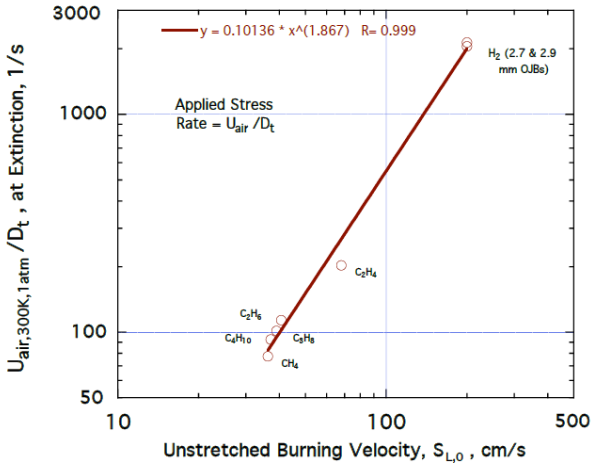

Figure 6. Comparison between extinction limits and laminar flame speed (Pellett, 2007).

By extrapolating the blow-off line from Fig. 5, an approximate ejection velocity of 800 cm/s is obtained for a fuel mole fraction of 20% silane/H2 mixture. Additionally, by applying the logarithmic equation from Fig. 6, the experimental laminar flame speed of the 20% silane/H2 mixture was determined. The calculation is expressed in Eq. (2) and Eq. (3).

$$\frac{Uair}{Dtube_{20\%\frac{SiH4}{H2}}} = \frac{800\left(\frac{cm}{s}\right)}{0{,}27(cm)} = \left(\frac{1}{s}\right), \tag{2}$$

$$SL_{20\%\frac{SiH4}{H2}} = \sqrt[1.867]{\frac{1}{0.10136}\frac{Uair}{Dtube_{20\%\frac{SiH4}{H2}}}} = 246{,}55\,\frac{cm}{s} \approx 2{,}47\,\frac{m}{s}, \tag{3}$$

The Silane_v3 mechanism laminar flame velocity calculated shown in Fig. 7 gives the value around 2,64 m/s to stoichiometric fuel equivalence ratio, with an error of 7% compared to the literature. This comparison between the calculated and experimental laminar flame speeds provides a means to validate the accuracy and predictive capabilities of the Silane_v3 mechanism in capturing the combustion characteristics of the silane-hydrogen-air system.

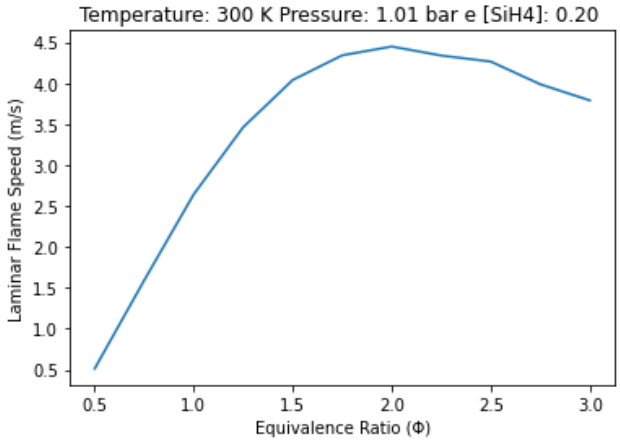

Figure 7. Validation Laminar Flame Speed of Silane/H2/air from Silane_v3.

Therefore, the validation of the mechanism for the analysis of the laminar flame speed of the silane/hydrogen/air mixture is satisfied for the ambient conditions, temperature of 300 K and pressure of 1 atm.

3. RESULTS AND DISCUSSION

This section presents the validation results of the Silane_v3 mechanism, focusing on the ignition delay time and laminar flame speed parameters collected from literature sources. Additionally, an in-depth analysis of these combustion parameters in the silane-hydrogen mixture under the operational conditions of the studied engine will be discussed.

3.1 Motor operation analysis

3.1.1 Ignition delay time

The Ignition Delay Time (Tau) was computed by considering the stoichiometry of the reaction and the specific operating conditions of the investigated engine (T=1100 K and P=1 atm) as shown in Fig. 8. This parameter represents the time interval between the initiation of the combustion process and the peak of OH formation.

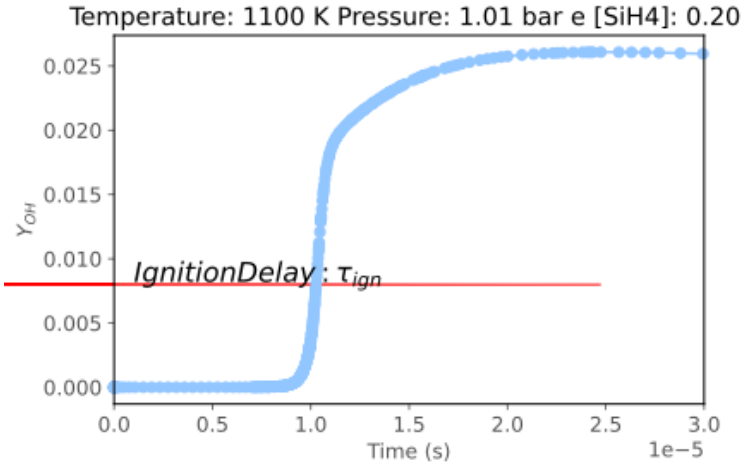

Figure 8. Ignition Delay Time of SiH4-H2-Air at T = 1100K and P = 1 atm.

From Fig. 9, the relationship between Tau and temperature is depicted as 10000/T(K), where T represents the temperature. It can be observed that the combustion of the Silane, Hydrogen, and Air mixture follows the Arrhenius equation within the temperature range of 550 to 1100 K. The Arrhenius equation describes the temperature dependence of reaction rates, and its applicability to the combustion process indicates that the reaction kinetics are consistent with a temperature-dependent exponential relationship.

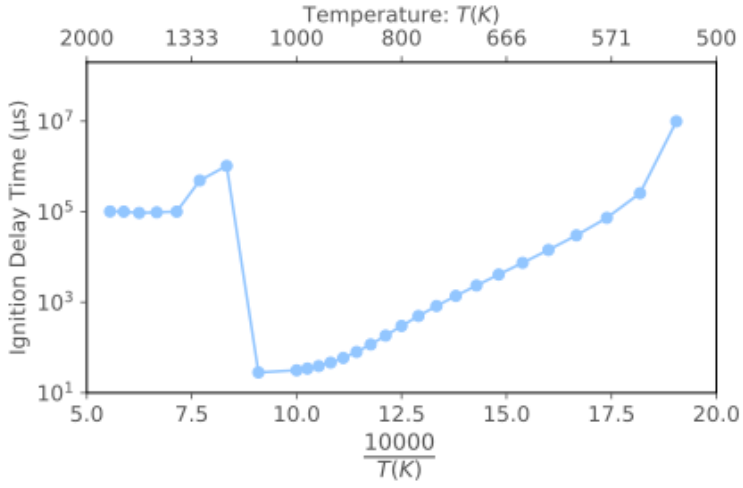

Figure 9. Ignition Delay Time of SiH4-H2-Air at P = 1 atm and Phi = 1.

3.1.2 Laminar flame speed

The calculation of the laminar flame speed using the Silane_v3 mechanism is presented at a reduced temperature compared to the operating conditions of the scramjet engine. The mechanism has been validated for low-temperature values. Hence, Fig. 10 shows the laminar flame speed values at a temperature of 600 K and pressure of 1 atm.

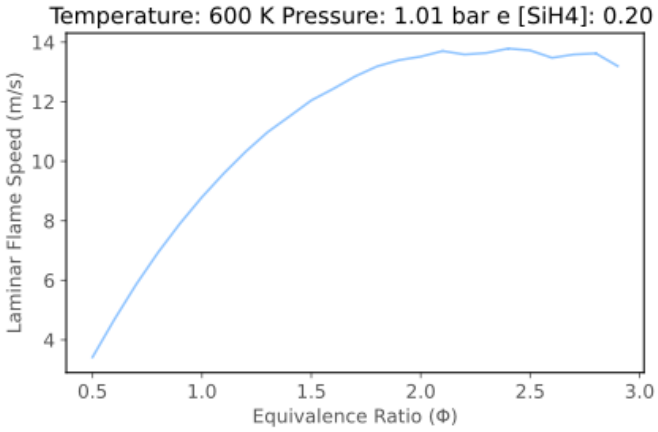

Figure 10. Laminar Flame Speed of Silane/H2/air from Silane_v3.

It was found that adjustments to the transport parameters and reaction rate constants involved in the model are required to accurately match the experimental data of the laminar flame speed. Further research and refinement of the mechanism are necessary to improve its predictive capabilities for high-temperature values.

3.1.3 Combustion emission

The primary emission to be analyzed is related to the NOx group, as the studied chemical kinetics mechanism does not include the emission of other pollutants as byproducts of the combustion of SiH4/H2/Air.

Additionally, the emission of silica (SiO2) will also be examined. While silica itself is not considered a pollutant, it is released in a condensed and solid state, which can lead to wear and tear on the combustion chamber and exhaust structure of the engine. Figure 11 presents the emissions of NOx products and Fig. 12 shows the production of silica as determined by the diffusive flame analysis.

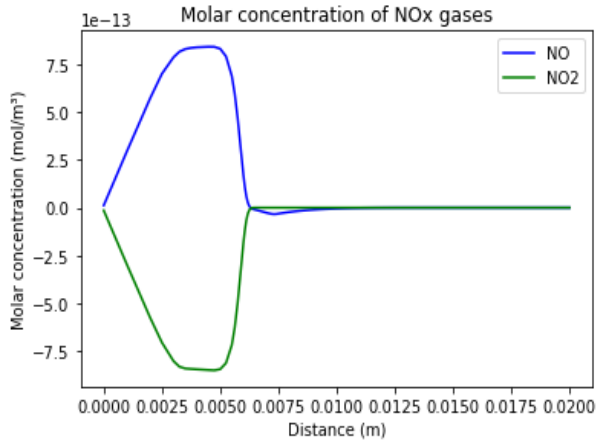

Figure 11. Emission of NOx products.

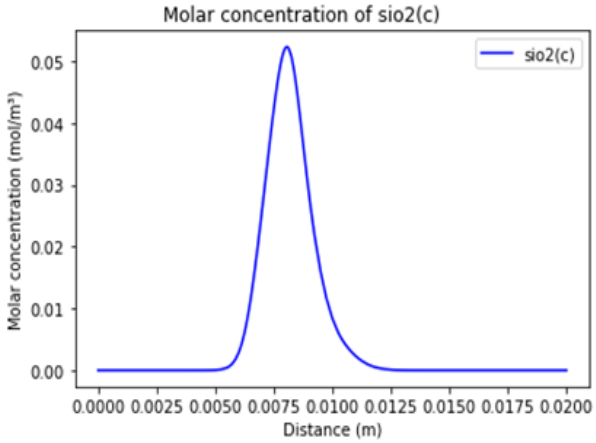

Figure 12. Production of silica.

The experimental data indicated the concurrent production of NO gas and the consumption of NO2 gases during the combustion process. Notably, these chemical species were observed at relatively low molar concentrations per cubic meter, signifying their involvement in the complex combustion chemistry. On the other hand, the prominent presence of silica as one of the principal combustion products highlights its significant role in the combustion of the silane/hydrogen/air mixture.

4. CONCLUSION

In conclusion, the chemical kinetics mechanism developed in this project demonstrated good agreement with the literature data for the ignition delay time calculation. However, when validating the mechanism using the extinction data of the studied mixture for the calculation of laminar flame speed, a significant error was observed for high temperature values. This discrepancy is likely attributed to the estimated transport parameters of some silane chemical species, as no experimental data were found in the literature. In addition, the reaction constants should be updated to cover the higher temperature combustion values.

The investigation yielded significant insights into the laminar flame speed behavior concerning temperature variations, revealing a remarkable threefold augmentation in the laminar flame speed value between 300K to 600K. Moreover, based on this analysis, it is reasonable to anticipate that this trend will endure as the temperature continues to rise, leading to a noteworthy increase in the laminar flame speed, which is projected to surpass 10 cm/s for temperatures exceeding 600K.

Furthermore, intriguing findings emerged with regards to the chemical composition of the combustion products. The examination of these emissions provides crucial insights into the environmental impact and potential wear on the engine components caused by the combustion process. By evaluating the emission levels of NOx and silica, it is possible to assess the environmental implications and operational considerations associated with the use of Silane-Hydrogen fuel systems.

However, further investigations and refinements in the chemical kinetics mechanism are warranted to precisely model the combustion behavior at elevated temperatures and accurately predict the laminar flame speed and pollutant emissions in such complex combustion scenarios.

5. REFERENCES

Anderson Jr., J. D. Modern Compressible Flow with Historical Perspective. 4th ed. [s.l.]: McGraw-Hill, 2020.

Bezzera, I. S. A., Numérica da Influência da Velocidade na Combustão Supersônica em um Demonstrador Scramjet. Dissertação de mestrado. Universidade Federal do Rio Grande do Norte, 2020.

Carneiro, R. Estudo Analítico de um Demonstrador da Tecnologia da Combustão Supersônica. Dissertação de mestrado. Universidade Federal do Rio Grande do Norte, 2020.

Cone, P. P. Assessing the Influence of Hypersonic Weapons on Deterrence. The Counterproliferation Papers. Future Warfare Series No. 59. June 2019.

Dong, Chen et al. Experimental study on the laminar flame speed of hydrogen/natural gas/air mixtures. State Key Laboratory of Multiphase Flow in Power Engineering, Xi'an Jiaotong University, Xi'an 710049, China. © Higher Education Press and Springer-Verlag Berlin Heidelberg, 2010.

FAB Notícias. Indústria Aeroespacial: O Brasil na era da Propulsão Hipersônica: Projeto 14-X. Available: fab.mil.br/noticias/mostra/38356/IND%C3%9ASTRIA%20AEROESPACIAL%20%20-%20O%20Brasil%20na%20era%20da%20Propuls%C3%A3o%20Hipers%C3%B4nica:%20Projeto%2014-X. Accessed 08 October2023.

Kraska, J., Pedrozo, R. Disruptive Technology and the Law of Naval Warfare. Oxford University Press, 2022.

Miller, J. A. et al. A comprehensive mechanism for silane pyrolysis and combustion. In: 32nd International Symposium on Combustion. The Combustion Institute, 2008. p. 263-270.

McLain, T. F. et al. A kinetic study of the ignition of silane in mixtures of hydrogen and oxygen. In: 1983 National Aerospace and Electronics Conference. Proceedings of the IEEE 1983 National Aerospace and Electronics Conference, Dayton, OH, USA, 1983. p. 84-88.

NASA. MSIS-E-90: A Computerized Model of the Earth's Atmosphere from Ground to Space (version 1990). Available: ccmc.gsfc.nasa.gov/modelweb/models/msis_vitmo.php. Accessed 16 May2023.

Jachimowski, C. J. Silane combustion. Combustion Science and Technology, v. 30, n. 1-6, p. 253-267, 1983.

Pellett, G. L.; Northam, G. B. Counterflow Diffusion Flames of Hydrogen, and Hydrogen Plus Methane, Ethylene, Propane, and Silane, vs. Air: Strain Rates at Extinction. NASA Langley Research Center, Hampton, Virginia, 1991.

Pellett, G. L.; Vaden, S. N.; Wilson, L. G. Opposed Jet Burner Extinction Limits: Simple Mixed Hydrocarbon Scramjet Fuels vs Air. In: 43rd AIAA/ASME/SAE/ASEE Joint Propulsion Conference & Exhibit. AIAA 2007-5664. 8-11 July, 2007, Cincinnati, Ohio.

UC San Diego. The San Diego Mechanism. [Online]. Available: web.eng.ucsd.edu/mae/groups/combustion/mechanism.html. Accessed 09July 2023.

6. RESPONSIBILITY NOTICE

The authors are the only responsible for the printed material included in this paper.

7. APPENDIX A

Table A1. List of Species of the Silane_v3 Kinetic Mechanism.

ID	Specie	ID	Specie
1	SiH2	20	H
2	O	21	HO2
3	H2	22	OH
4	H2O	23	H2SiOH
5	H3SiSiH3	24	H3SiOO
6	Si(OH)2	25	Si2H2
7	N2	26	Si2
8	SiO2(c)	27	HOSiO
9	SiH4	28	SiH3
10	HSiO(OH)	29	SiH
11	Si2H5	30	H3SiSiH
12	Si	31	Si2O2
13	Si2H3	32	H2SiSiH2
14	H2SiO	33	HSiOH
15	SiO	34	O2
16	C-OSiH2O	35	N
17	HSiO	36	NO
18	H2O2	37	NO2
19	Si3	-	-

Table A2. List of Reactions of the Silane_v3 Kinetic Mechanism.

ID	Equation	ID	Equation	ID	Equation
1	OH + SiO <=> H + sio2(c)	26	SiH + SiH2 <=> Si2H3	51	H3SiSiH3 <=> H2 + H3SiSiH
2	Si(OH)2 <=> H2O + SiO	27	H + Si2H2 <=> Si2H3	52	SiH + SiH4 <=> SiH2 + SiH3
3	H + SiH4 <=> H2 + SiH3	28	H + OH + M <=> H2O + M	53	O + SiO + M => sio2(c) + M
4	H2 + SiH <=> SiH3	29	O2 + SiH2 <=> HSiO + OH	54	H + Si(OH)2 <=> H2 + HOSiO
5	H + O2 <=> O + OH	30	HSiO <=> H + SiO	55	H2SiO + SiO => H2 + Si2O2
6	H2 + OH <=> H + H2O	31	HSiOH <=> H2 + SiO	56	H + O2 + M <=> HO2 + M
7	H2 + O <=> H + OH	32	H2O + SiH2 <=> H2 + HSiOH	57	H + O2 (+N2) <=> HO2 (+N2)
8	SiH4 (+M) <=> H2 + SiH2 (+M)	33	OH + SiH4 => H2O + SiH3	58	H2 + Si2H2 <=> H3SiSiH
9	H2 + H2SiSiH2 <=> SiH2 + SiH4	34	Si + Si3 <=> 2 Si2	59	Si2O2 <=> 2 SiO
10	O2 + SiO => O + sio2(c)	35	2 OH <=> H2O + O	60	H3SiOO (+M) <=> C-OSiH2O + H (+M)
11	H + sio2(c) <=> HOSiO	36	2 SiH2 <=> H2 + Si2H2	61	H3SiSiH3 <=> SiH2 + SiH4
12	H2 + Si2H2 <=> H2SiSiH2	37	H2 + Si2H3 <=> Si2H5	62	H3SiSiH <=> H2SiSiH2
13	C-OSiH2O <=> HSiO(OH)	38	H2 + Si3 <=> Si + Si2H2	63	HSiO + OH <=> H2O + SiO
14	O2 + SiH3 <=> C-OSiH2O + H	39	H + HSiO <=> H2 + SiO	64	H2 + O2 <=> H + HO2
15	HSiO(OH) <=> Si(OH)2	40	H + HO2 <=> 2 OH	65	Si2 + SiH2 <=> H2 + Si3
16	Si(OH)2 <=> H + HOSiO	41	H2SiOH <=> H2 + HSiO	66	HSiO(OH) + O2 <=> H + HO2 + sio2(c)
17	O2 + Si <=> O + SiO	42	H2O + SiH2 => H + H2SiOH	67	H2O2 + M <=> 2 OH + M
18	H2 + Si2 <=> 2 SiH	43	SiH + SiH4 <=> Si2H5	68	O2 + SiH4 <=> HO2 + SiH3
19	H2 + M <=> 2 H + M	44	H + O2 + H2O <=> HO2 + H2O	69	H + H2O2 <=> H2O + OH
20	H2 + H2SiSiH2 <=> H3SiSiH3	45	SiH3 + SiH4 <=> H2 + Si2H5	70	H + H2SiO <=> H2 + HSiO
21	H2 + Si2 <=> Si2H2	46	O + SiH4 <=> OH + SiH3	71	N + O2 <=> NO + O
22	Si + SiH2 <=> Si2H2	42	H + HSiO(OH) <=> H2 + HOSiO	72	HO2 + NO <=> NO2 + OH
23	HSiO(OH) <=> H + HOSiO	48	O2 + SiH3 <=> H2SiO + OH	73	NO2 + O <=> NO + O2
24	SiH2 + M <=> H2 + Si + M	49	H + O + M <=> OH + M	74	NO2 + H <=> NO + OH
25	OH + SiO <=> HOSiO	50	O2 + SiH3 (+M) <=> H3SiOO (+M)	-	-

8. APPENDIX B

Table B1. Species Transport Properties of the Silane_v3 Kinetic Mechanism.

ID	Specie	Model	Geometry	Diameter	Well-depth	Data Source
1	SiH2	gas	nonlinear	3.803	133.10	San Diego, 2023
2	O	gas	atom	2.750	80.00	San Diego, 2023
3	H2	gas	linear	2.920	38.00	San Diego, 2023
4	H2O	gas	nonlinear	2.605	572.40	San Diego, 2023
5	H3SiSiH3	gas	nonlinear	4.828	301.30	San Diego, 2023
6	Si(OH)2	gas	nonlinear	4.800	170.60	Estimation by HCOOH (San Diego)
7	N2	gas	linear	3.621	97.53	Estimation by CO2 (San Diego)
8	SiO2(c)	gas	nonlinear	4.270	316.11	San Diego, 2023
9	SiH4	gas	nonlinear	4.084	207.60	Estimation by HCOOH (San Diego)
10	HSiO(OH)	gas	nonlinear	5.000	609.69	San Diego, 2023
11	Si2H5	gas	nonlinear	4.717	306.90	San Diego, 2023
12	Si	gas	atom	2.910	3036.00	San Diego, 2023
13	Si2H3	gas	nonlinear	4.494	318.20	San Diego, 2023
14	H2SiO	gas	nonlinear	4.070	645.19	Estimation by HCO (San Diego)
15	SiO	gas	linear	4.140	127.09	Estimation by CO (San Diego)
16	C-OSiH2O	gas	nonlinear	5.000	430.00	Estimation by HOCH2O (San Diego)
17	HSiO	gas	nonlinear	4.070	645.19	Estimation by HCO (San Diego)
18	H2O2	gas	nonlinear	3.458	107.40	San Diego, 2023
19	Si3	gas	nonlinear	3.550	3036.00	San Diego, 2023
20	H	gas	atom	2.050	145.00	San Diego, 2023
21	HO2	gas	nonlinear	3.458	107.40	San Diego, 2023
22	OH	gas	linear	2.750	80.00	San Diego, 2023
23	H2SiOH	gas	nonlinear	4.190	540.25	Estimation by CH2OH (San Diego)
24	H3SiOO	gas	nonlinear	4.110	624.20	Estimation CH3O2 (San Diego)
25	Si2H2	gas	nonlinear	4.383	323.80	San Diego, 2023
26	Si2	gas	linear	3.280	3036.00	San Diego, 2023
27	HOSiO	gas	nonlinear	4.070	645.19	Estimation by OCHO (San Diego)
28	SiH3	gas	nonlinear	3.943	170.30	San Diego, 2023
29	SiH	gas	linear	3.662	95.80	San Diego, 2023
30	H3SiSiH	gas	nonlinear	4.601	312.60	San Diego, 2023
31	Si2O2	gas	nonlinear	4.500	564.87	Estimation by HCCOH (San Diego)
32	H2SiSiH2	gas	nonlinear	4.601	312.60	San Diego, 2023
33	HSiOH	gas	nonlinear	4.070	645.19	Estimation by HCOH (San Diego)
34	O2	gas	linear	3.458	107.40	San Diego, 2023
35	N	gas	atom	3.298	71.40	San Diego, 2023
36	NO	gas	linear	3.621	97.53	San Diego, 2023
37	NO2	gas	nonlinear	3.500	200.00	San Diego, 2023